# Extended Ground Distance Relaying With Fault Resistance Compensation

Diogo de Oliveira Fialho Pereira
Electrical Engineering Department
Federal University of Rio Grande do Sul
90035-190 Porto Alegre, RS, Brazil
Email: diogo@ece.ufrgs.br

Arturo Suman Bretas
Electrical Engineering Department
Federal University of Rio Grande do Sul
90035-190 Porto Alegre, RS, Brazil
Email: abretas@ece.ufrgs.br

***Abstract*—Fault resistance introduces an error in traditional ground distance relay apparent impedance measurement process. If not accordingly considerated it produces primary protection zone underreach. Line asymmetry also affects relay operation producing overreaching. So due to these two aspects protection zone limits of ground distance relays present low precision. In order to increase these precision limits, a new protection algorithm is proposed. The proposed method is based in phase coordinates and uses a fault resistance estimate to develop the trip decision procedure. The estimation procedure uses one-terminal voltage and current data in an iterative process. The proposed algorithm results are compared to traditional ground distance relay for method validation.**

***Index Terms*—Fault diagnosis, fault resistance, power system faults, power system protection, protective relaying.**

## I. Introduction

Distance relays are devices widely used in transmission line protection. The principle of operation of such protection devices is the comparison of the apparent impedance of one line terminal with a relay operation characteristic based on the line parameters to decide between line trip or not. The apparent impedance comparison procedure occurs after the fault detection. This method presents acceptable precision for low resistance faults once the effective impedance between the relay and the fault location nearly reaches the apparent impedance measured by the relay [1].

Fault resistance introduces an error in the fault distance estimate since the apparent impedance measured in the relay terminal is no longer necessarily proportional to the line length between the relay and the fault position [2].

To mitigate the fault resistance effect in the fault distance estimate several methods are proposed. For traditional distance relays this compensation is obtained with a quadrilateral characteristic dependent of the angle between the fault current contribution from the remote and the sending end of the line [3]. The use of a quadrilateral characteristic produces a better fault resistance coverage and arc compensation. Several types of distance relay characteristics are available for the same purpose [3]–[6]. These alternative impedance relays, however, have the disadvantage of affecting the loadability of the relay for high resistance faults [2].

The authors would like to thank Conselho Nacional de Desenvolvimento Científico e Tecnológico (CNPq) for the financial support received.

The fault resistance estimation is presented in [7]–[11] as a way to compensate for this limitation. These works include a fault resistance estimate and compensation in the tripping decision process resulting in a higher accuracy in the distance relay operation. The fault resistance estimation is accomplished using symmetrical or modal components, which restricts their application for balanced system with equally transposed lines.

In [12], the fault resistance is estimated based on phase components. However, the equations are developed for unbalanced systems considering a passive remote end, limiting the methods online application.

This work presents a distance relaying fault resistance compensation technique based on phase-coordinates considering fault current feeding from both ends of the line. The fault resistance estimation procedure utilizes one-terminal voltage and current data in an iterative process. The procedure is applicable for systems with transposed and nontransposed lines. The fault resistance is considered constant during the fault occurrence. The results obtained with the new method are compared with the traditional ground distance relay for trip procedure efficiency improvement demonstration.

## II. Ground distance relaying with fault resistance compensation

In this section, a distance relaying algorithm for a line-to-ground fault is developed using phase-coordinates and considering the fault resistance.

Referring to Fig. 1, which shows a single line-to-ground fault (A-g), the fault point voltage, $V_{F_a}$, is given by (1):

$$V_{F_a} = V_{S_a} - x \cdot [Z_a] \cdot [I_S] \tag{1}$$

where $V_{S_a}$ is the phase $a$ voltage at the relay point, $[Z_a]$ is the phase $a$ impedance vector, $x$ is the distance between the relay and the fault point and $[I_S]$ is the relay point currents vector.

Expanding (1), (2) is obtained:

$$V_{F_a} = V_{S_a} - x \cdot (Z_{aa} \cdot I_{S_a} + Z_{ab} \cdot I_{S_b} + Z_{ac} \cdot I_{S_c}) \tag{2}$$

$$= R_F \cdot I_{F_a} \tag{3}$$

where $R_F$ is the fault resistance and $I_{F_a}$ is the fault current, given by the relation between the sending and remote-end

currents:

$$I_{F_a} = I_{S_a} + I_{R_a} \tag{4}$$

Using (2) to (4), it is possible to obtain (5):

$$V_{S_a} = R_F \cdot (I_{R_a} + I_{S_a}) + x \cdot (Z_{aa} \cdot I_{S_a} + Z_{ab} \cdot I_{S_b} + Z_{ac} \cdot I_{S_c}) \tag{5}$$

The apparent impedance at the sending-end of the line, where the relay is located, is given by (6):

$$Z_{m_{ap}} = \frac{V_{S_a}}{I_{S_a}} \tag{6}$$

Using (5) and (6), the measured apparent impedance, $Z_{m_{ap}}$, can be rearranged to (7):

$$Z_{m_{ap}} = x \cdot \left[ Z_{aa} + Z_{ab} \frac{I_{S_b}}{I_{S_a}} + Z_{ac} \frac{I_{S_c}}{I_{S_a}} \right] + R_F \cdot \left[ 1 + \frac{I_{R_a}}{I_{S_a}} \right] \tag{7}$$

From (7), the measured apparent impedance is given by two distinct components. The second term in the right side of (7) represents the fault resistance effect in the measured apparent impedance. Clearly, the fault resistance effect is not only determined by its value, but also by the relation of the sending and remote-end currents during the fault.

The first term in the right side of the equation represents the impedance of the line section between the relay point and the fault. The phase-coordinates approach shows that this impedance depends on the three-phase currents, due to mutual coupling. For transposed lines and balanced loads, this term can be simplified to $x \cdot Z_{aa}$, which represents the self impedance of the faulted phase.

In order to improve the robustness and precision of the proposed method, the nonfaulted phases effect must be considered.

The proposed scheme settings are:

- $\ell$, the total line length;
- $p$, the line length percentage to be protected;
- $[Z]$, the line impedance matrix;

During a fault, the three-phase currents are measured online and the impedance setting is determined by the line length to be protected. With this setting, the measured impedance can be compared in order to determine the trip decision.

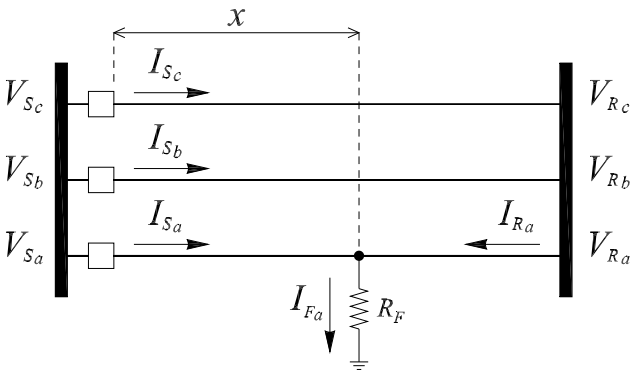


Fig. 1. Faulted transmission line

Rearranging (7), the final equation for the proposed ground distance relay is obtained:

$$\ell \cdot p \cdot \left[ Z_{aa} + Z_{ab} \frac{I_{S_b}}{I_{S_a}} + Z_{ac} \frac{I_{S_c}}{I_{S_a}} \right] = Z_{m_{ap}} - R_F \cdot \left[ 1 + \frac{I_{R_a}}{I_{S_a}} \right] \tag{8}$$

During fault occurrence, the left term in (8) is determined by the measured currents and the relay settings. Then, the measured impedance $Z_{m_{ap}}$ is compensated with the fault resistance estimate (whose algorithm is covered in the next section) to reach the final trip decision.

## III. Fault Resistance Estimation Using Phase Coordinates

### A. Mathematical Development

Referring to Fig. 1, which shows an A-g fault, the voltages measured at the relay point are given by (9):

$$\begin{bmatrix} V_{S_a} \\ V_{S_b} \\ V_{S_c} \end{bmatrix} = x \cdot \begin{bmatrix} Z_{aa} Z_{ab} Z_{ac} \\ Z_{ba} Z_{bb} Z_{bc} \\ Z_{ca} Z_{cb} Z_{cc} \end{bmatrix} \cdot \begin{bmatrix} I_{S_a} \\ I_{S_b} \\ I_{S_c} \end{bmatrix} + \begin{bmatrix} V_{F_a} \\ V_{F_b} \\ V_{F_c} \end{bmatrix} \tag{9}$$

where:

| | |
|---|---|
| $V_{S_{a,b,c}}$ | sending-end phase voltages [V] |
| $x$ | distance between the relay and the fault point $[km]$ |
| $Z_{mm}$ | phase $m$ self impedance $[\Omega/km]$ |
| $Z_{mn}$ | mutual impedance between phases $m$ and $n$ $[\Omega/km]$ |
| $I_{S_{a,b,c}}$ | sending-end phase currents [A] |
| $V_{F_{a,b,c}}$ | fault point phase voltages [V] |

For an A-g fault, the faulted phase voltage at the sending-end is given by (10):

$$V_{S_a} = V_{F_a} + x \cdot [Z_{aa} I_{S_a} + Z_{ab} I_{S_b} + Z_{ac} I_{S_c}] \tag{10}$$

where $V_{F_a} = R_F \cdot I_{F_a}$, in which $R_F$ represents the fault resistance and $I_{F_a}$ is the phase $a$ fault current.

Assuming that the fault impedance is strictly resistive and constant during the analyzed period, it is possible to arrange (10) into its real and imaginary parts, resulting in (11) and (12), respectively:

$$V_{S_{a_r}} = x \cdot M_1 + R_F \cdot I_{F_{a_r}} \tag{11}$$

$$V_{S_{a_i}} = x \cdot M_2 + R_F \cdot I_{F_{a_i}} \tag{12}$$

where the subscript indices $r$ and $i$ represent, respectively, the real and imaginary parts of the components and

$$M_1 = Z_{aa_r} I_{S_{a_r}} - Z_{aa_i} I_{S_{a_i}} + Z_{ab_r} I_{S_{b_r}} - Z_{ab_i} I_{S_{b_i}} + Z_{ac_r} I_{S_{c_r}} - Z_{ac_i} I_{S_{c_i}} \tag{13}$$

$$M_2 = Z_{aa_r} I_{S_{a_i}} + Z_{aa_i} I_{S_{a_r}} + Z_{ab_r} I_{S_{b_i}} + Z_{ab_i} I_{S_{b_r}} + Z_{ac_r} I_{S_{c_i}} + Z_{ac_i} I_{S_{c_r}} \tag{14}$$

It is possible to arrange (11) and (12) into a matrix form, as (15):

$$\begin{bmatrix} V_{S_{a_r}} \\ V_{S_{a_i}} \end{bmatrix} = \begin{bmatrix} M_1 & I_{F_{a_r}} \\ M_2 & I_{F_{a_i}} \end{bmatrix} \begin{bmatrix} x \\ R_F \end{bmatrix} \tag{15}$$

In (15), the sending-end voltages are function of the fault distance and the fault resistance. It is possible to obtain (16), where the fault distance and its resistance depend on the sending-end voltages and currents, as well as the line parameters, $M_1$ and $M_2$:

$$\begin{bmatrix} x \\ R_F \end{bmatrix} = \frac{1}{M_1 I_{F_{a_i}} - M_2 I_{F_{a_r}}} \begin{bmatrix} I_{F_{a_i}} & -I_{F_{a_r}} \\ -M_2 & M_1 \end{bmatrix} \begin{bmatrix} V_{S_{a_r}} \\ V_{S_{a_i}} \end{bmatrix} \quad (16)$$

From (16) the fault resistance and the fault distance are independent and its expressions are given by (17) and (18):

$$x = \frac{I_{F_{a_i}} V_{S_{a_r}} - I_{F_{a_r}} V_{S_{a_i}}}{M_1 I_{F_{a_i}} - M_2 I_{F_{a_r}}} \quad (17)$$

$$R_F = \frac{-M_2 V_{S_{a_r}} + M_1 V_{S_{a_i}}}{M_1 I_{F_{a_i}} - M_2 I_{F_{a_r}}} \quad (18)$$

Based in (17) and (18) it is possible to obtain the fault distance and the fault resistance from the parameters of the system, the fault current and the sending-end voltages. These variables are previously known, and an iterative procedure that updates the fault current is used to estimate the fault resistance.

### *B. Fault Current Estimation Procedure*

In (18) the only unknown variable is the fault current phasor $I_{F_{a_{r,i}}}$. All other variables are system's parameters or measured variables.

Referring to Fig. 1, the fault current can be obtained by (21):

$$I_{F_a} = I_{S_a} + I_{R_a} \quad (21)$$

where $I_{R_a}$ is the phase $a$ remote-end current.

Since remote-end current during the fault is different from the pre-fault current the follow iterative technique is used to estimate the load current during the fault [13]:

1) Remote-end current, $I_{R_a}$, during the fault is assumed to be the same as the pre-fault remote-end current;
2) Fault current is calculated using (21);
3) Fault location and fault resistance are estimated by (17) and (18);
4) Remote-end current ($I_{R_a}$) is updated using (22):

$$I_{R_a} = \frac{V_{S_a} - V_{R_a} - x Z_a I_s}{(\ell - x) Z_{aa}} - \frac{Z_{ab}}{Z_{aa}} I_{S_b} - \frac{Z_{ac}}{Z_{aa}} I_{S_c} \quad (22)$$

   where $V_{R_a}$ is the remote-end estimated voltage calculated by $V_{R_a} = V + Z I_{R_a}$ where $V$ and $Z$ are the faulted phase voltage and impedance estimated with the pre-fault conditions;
5) Check if $R_F$ converges, using (23):

$$|R_F(n) - R_F(n-1)| < \delta \quad (23)$$

   where $\delta$ is a previously defined threshold value.
6) If $R_F$ converged, stop the procedure, otherwise, go back to step II.

The outputs of this procedure are the fault resistance ($R_F$) and the remote-end current. These values are used in (8), along with the known values of the line impedance, the measured sending-end voltages and currents, the estimated receiving-end fault voltages and also the proposed distance relay settings values.

## IV. Case Study

For the proposed method validation, several fault cases were simulated using ATP/EMTP [14]. The system operates in 60 Hz and has a total line length of 108 km, with its impedance matrix given inicialy by (19) in the first five cases presented, and by (20) in the five last cases. To analyze the tests results, an admittance ($mho$) characteristic distance relay, whose first zone is set at 85% of the line impedance (91.8 kilometers distant from the relay location), is used. The voltages and currents data are measured at the relay location using a sampling rate of 192 samples per cycle and the phasors are estimated using a half-cycle Fourier filter [15].

In the following figures presented, the apparent impedance trajectories estimated with the proposed algorithm, are represented by the solid line, whereas the dashed lines show the apparent impedance trajectories given by the traditional ground distance relay, using $Z_{apparent} = E_a / I'_a$, where $I'_a$ is given by (24) [2]:

$$I'_a = I_a + m I_0 = I_a + \frac{Z_0 - Z_1}{Z_1} I_0 \quad (24)$$

where $m$ is the compensation factor, $I_0$ is the zero sequence current measured at the sending-end, $Z_0$ and $Z_1$ are the zero and positive sequence line impedances, respectively.

Since the analyzed test case also considers an asymmetric line configuration, $Z_0$ and $Z_1$ are given by (25) and (26), respectively:

$$Z_0 = Z_{a_0} + 2 Z_{ab_0} \quad (25)$$

$$Z_1 = Z_{a_0} - Z_{ab_0} \quad (26)$$

where

$$Z_{a_0} = \frac{1}{3} \cdot (Z_{aa} + Z_{bb} + Z_{cc}) \quad (27)$$

$$Z_{ab_0} = \frac{1}{3} \cdot (Z_{ab} + Z_{bc} + Z_{ca}) \quad (28)$$

Figs. 2 to 6 present the results of the algorithm in a transposed line defined by (19). For the Figs. 2 to 4 the fault resistance is $R_F = 100\ \Omega$, and the fault distance 87.5%, 81.25% and 50% respectively. Fig 2 presents an external fault test case whereas Figs. 3 and 4 show internal faults. In all the three test cases the proposed ground distance relay operated correctly. The tradicional relay however consider in all scenarios the faults external to the primary protection zone.

Fig. 5 show a less critical scenario where the fault resistance is equal to $R_F = 50\ \Omega$ and the faul distance equal to the half of the line length. Even in this situation the tradicional relay was unable to correctly characterize the fault. Once again the proposed method was successful.

In Figs. 6 and 7 it is presented an external fault condition whith the fault resistance equal to $R_F = 0\ \Omega$. While in the Fig. 6 the line is transposed, in the Fig. 7 the line is untransposed.

$$Z_{line} = \begin{bmatrix} 0,3192 + j0,95 & 0,0849 + j0,45 & 0,0849 + j0,45 \\ 0,0849 + j0,45 & 0,3192 + j0,95 & 0,0849 + j0,45 \\ 0,0849 + j0,45 & 0,0849 + j0,45 & 0,3192 + j0,95 \end{bmatrix} \Omega/km \quad (19)$$

$$Z_{line} = \begin{bmatrix} 0,31920 + j0,950 & 0,07641 + j0,405 & 0,08490 + j0,450 \\ 0,07641 + j0,405 & 0,31920 + j0,950 & 0,09339 + j0,495 \\ 0,08490 + j0,450 & 0,09339 + j0,495 & 0,31920 + j0,950 \end{bmatrix} \Omega/km \quad (20)$$

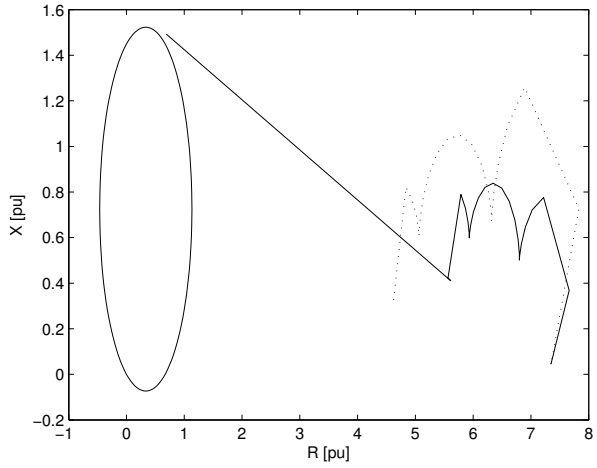


Fig. 2. Measured impedance trajectory for an A-g fault with $R_F = 100\ \Omega$ and $x = 94.5$ km (external fault)

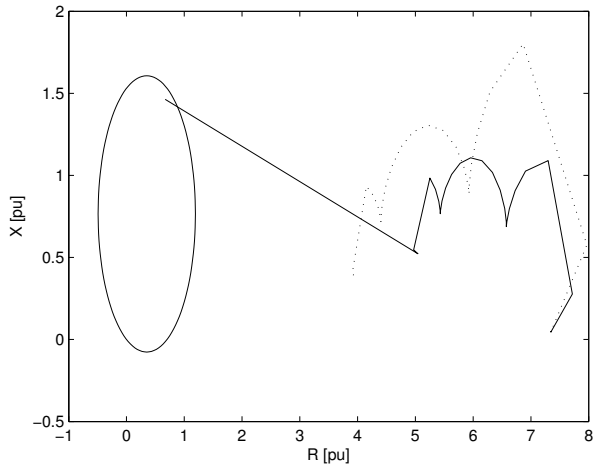


Fig. 3. Measured impedance trajectory for an A-g fault with $R_F = 100\ \Omega$ and $x = 87.75$ km (internal fault)

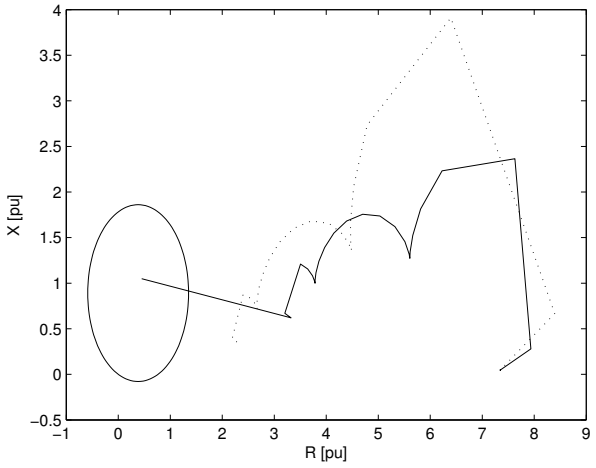


Fig. 4. Measured impedance trajectory for an A-g fault with $R_F = 100\ \Omega$ and $x = 54$ km (internal fault)

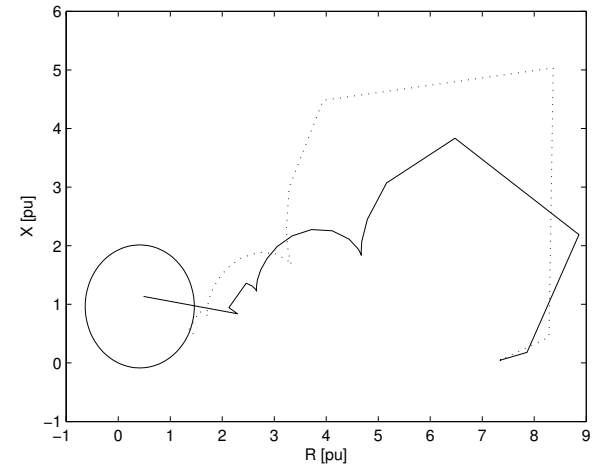


Fig. 5. Measured impedance trajectory for an A-g fault with $R_F = 50\ \Omega$ and $x = 54$ km (internal fault)

In both cases the proposed method operated correctly, whereas the tradicional relay defined the faults incorrectly as internal.

Figs. 8 and 9 show the impedance trajectory for faults with fault resistance $R_F = 100\ \Omega$ near the primary zone limit, where in Fig. 8 an internal fault test result is presented and Fig. 9 an external fault. The line is untransposed in both test cases, and the proposed ground distance relay operated correctly in both cases. Once again the tradicional relay was unable to determinate the internal fault.

For Figs. 10 and 11, as in the two previous cases, the line is untransposed with fault resistance equal to $R_F = 50\ \Omega$. The Fig. 10 presents a fault in the middle of the line and Fig. 11 an external fault close to the primary zone limit. The proposed method properly identified the faults, whereas the tradicional relay misoperated in the internal fault because the underreaching phenomenon due to fault resistance.

TABLE I
OVERVIEW OF THE RESULTS

| Case | Distance [km] | Apparent Impedance [Ω] | | Zone 1 | | Fault Resistance | | | N | Time [ms] |
|---|---|---|---|---|---|---|---|---|---|---|
| | | $\mathbf{Z_{m_{ap}}}$ | $\mathbf{Z_{traditional}}$ | Proposed | Traditional | Simulated | Estimated | Error | | |
| 1 | 94.5 | 26.22 + j56.86 | 178.2 + j11.98 | External | External | 100 | 99.73 | 0.27% | 6 | 5.99 |
| 2 | 87.75 | 25.55 + j55.74 | 151.9 + j14.46 | Internal | External | 100 | 99.88 | 0.12% | 4 | 6.41 |
| 3 | 54 | 17.15 + j39.93 | 87.35 + j13.36 | Internal | External | 100 | 99.98 | 0.02% | 4 | 5.95 |
| 4 | 54 | 18.54 + j43.20 | 56.00 + j18.45 | Internal | External | 50 | 49.99 | 0.02% | 4 | 5.96 |
| 5 | 94.5 | 41.24 + j80.94 | 22.14 + j47.26 | External | Internal | 0 | 0 | 0.00% | 3 | 6.05 |
| 6 | 94.5 | 38.77 + j80.82 | 39.09 + j40.99 | External | Internal | 0 | 0 | 0.00% | 3 | 6.21 |
| 7 | 87.75 | 23.15 + j58.56 | 165.3 + j4.449 | Internal | External | 100 | 99.85 | 0.15% | 5 | 5.95 |
| 8 | 94.5 | 23.58 + j60.15 | 191.4 + j3.176 | External | External | 100 | 99.67 | 0.33% | 6 | 6.14 |
| 9 | 54 | 17.45 + j43.97 | 66.14 + j3.516 | Internal | External | 50 | 49.99 | 0.02% | 4 | 5.98 |
| 10 | 94.5 | 26.37 + j65.04 | 146.9 + j0.740 | External | External | 50 | 49.90 | 0.02% | 6 | 5.99 |

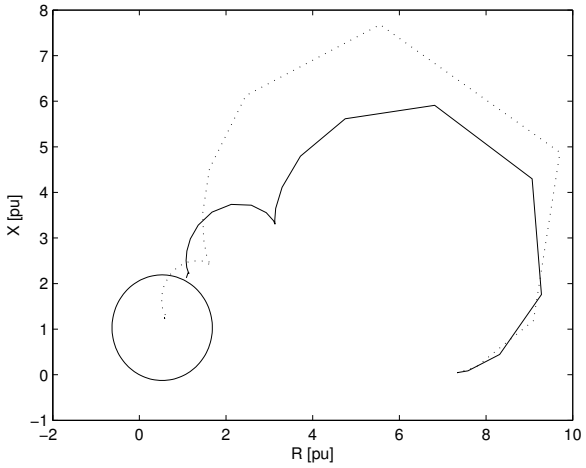


Fig. 6. Measured impedance trajectory for an A-g fault with $R_F = 0\ \Omega$ and $x = 94.5$ km (external fault)

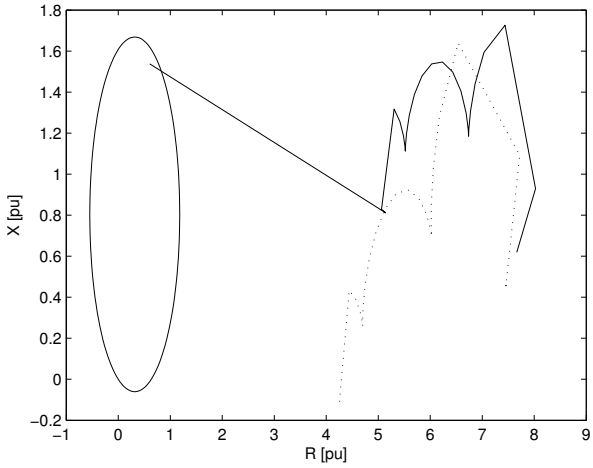


Fig. 8. Measured impedance trajectory for an A-g fault with $R_F = 100\ \Omega$ and $x = 87.75$ km (internal fault)

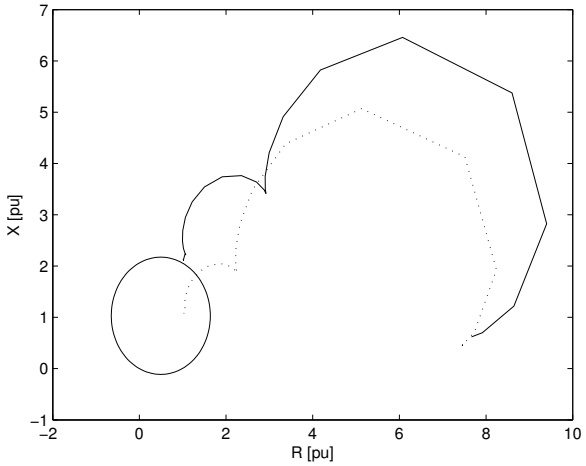


Fig. 7. Measured impedance trajectory for an A-g fault with $R_F = 0\ \Omega$ and $x = 94.5$ km (external fault)

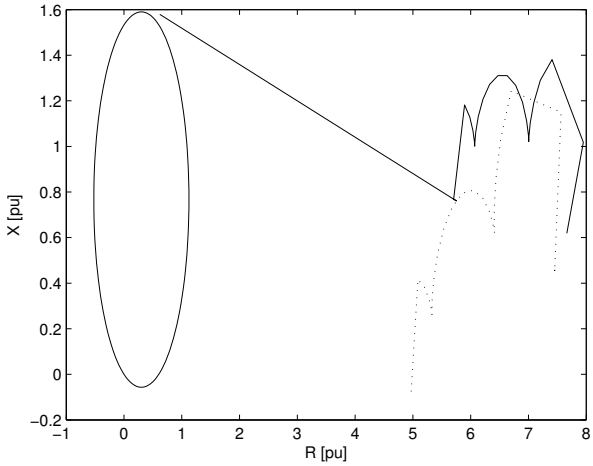


Fig. 9. Measured impedance trajectory for an A-g fault with $R_F = 100\ \Omega$ and $x = 94.5$ km (external fault)

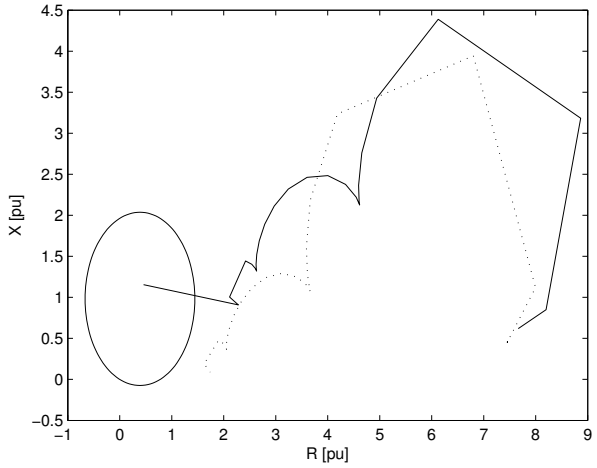


Fig. 10. Measured impedance trajectory for an A-g fault with $R_F = 50\ \Omega$ and $x = 54$ km (internal fault)

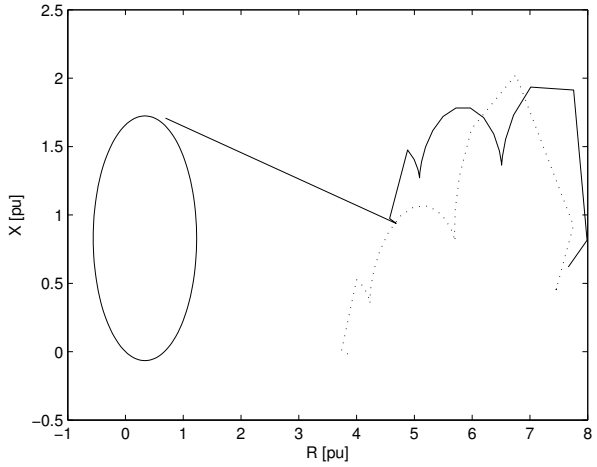


Fig. 11. Measured impedance trajectory for an A-g fault with $R_F = 50\ \Omega$ and $x = 94.5$ km (external fault)

Table I summarize the results presenting an overview of the cases analysed. Column one is the case number, column two the fault distance to the sending end. Column three and four are the apparent impedance measured by the proposed method and the tradicional relay, respectively. Column five show the primery zone decision for the proposed algorithm and column six for the tradicional relay. The fault resistance simulated and estimated are shown in columns seven and eight, and column nine show the relative error in the fault resistance estimation. Columns ten and eleven show, respectively, the number of iterations and the computacional time. The computacional time presented is obtained using Matlab in an ordinary PC.

## V. Conclusion

This paper proposes a new numerical distance algorithm based on phase coordinates and fault resistance estimation. The method is applicable to transposed and untransposed lines.

The results presented show the proposed methodology efficiency increase related to the tradicional ground distance relay. All the cases simulated were accordingly characterized related to the primary protection zone by the proposed method.

## References


[1] P. M. Anderson, *Power System Protection*. IEEE Press Power Engineering Series, 1999.

[2] S. Horowitz and A. Phadke, *Power System Relaying*. Research Studies Press, 1995.

[3] G. Ziegler, *Numerical Distance Protection*. Publicis Corporate Publishing, Erlang, 2006.

[4] Y. Xia, A. David, and K. Li, "High-resistance faults on a multi-terminal line: analysis, simulated studies and an adaptive distance relaying scheme," *IEEE Transactions on Power Delivery*, vol. 9, no. 1, pp. 492–500, Jan. 1994.

[5] K. K. Li and L. L. Lai, "Ideal operating region of digital distance relay under high resistance earth fault," *Electric Power Systems Research*, vol. 43, pp. 215–219, 1997.

[6] M. Erezzaghi and P. Crossley, "The effect of high resistance faults on a distance relay," in *Power Engineering Society General Meeting, 2003, IEEE*, vol. 4, 13-17 July 2003.

[7] D. L. Waikar, S. Elangovan, and A. Liew, "Fault impedance estimation algorithm for digital distance relaying," *IEEE Transactions on Power Delivery*, vol. 9, no. 3, pp. 1375–1383, July 1994.

[8] D. L. Waikar and P. S. M. Chin, "Fast and accurate parameter estimation algorithm for digital distance relaying," *Electric Power Systems Research*, vol. 4, pp. 53–60, 1998.

[9] D. L. Waikar, S. Elangovan, and A. Liew, "Further enhancements in the symmetrical components based improved fault impedance estimation method – Part I: Mathematical modelling," *Electric Power Systems Research*, vol. 40, pp. 189–194, 1997.

[10] D. L. Waikar, A. Liew, and S. Elangovan, "Further enhancements in the symmetrical components based improved fault impedance estimation method – Part II: Performance evaluation," *Electric Power Systems Research*, vol. 40, pp. 189–194, 1997.

[11] M. Eissa, "Ground distance relay compensation based on fault resistance calculation," *IEEE Transactions on Power Delivery*, vol. 21, no. 4, pp. 1830–1835, Oct. 2006.

[12] A. D. Filomena, R. H. Salim, M. Resener, and A. S. Bretas, "Ground distance relaying with fault-resistance compensation for unbalanced systems," *IEEE Transactions on Power Delivery*, 2008.

[13] S.-J. Lee, M.-S. Choi, S.-H. Kang, B.-G. Jin, D.-S. Lee, B.-S. Ahn, N.-S. Yoon, H.-Y. Kim, and S.-B. Wee, "An intelligent and efficient fault location and diagnosis scheme for radial distribution systems," *IEEE Transactions on Power Delivery*, vol. 19, no. 2, pp. 524–532, April 2004.

[14] Bonneville Power Administration, "Alternative Transient Program: ATP/EMTP," 2007. [Online]. Available: http://www.emtp.org/

[15] C.-S. Chen, C.-W. Liu, and J.-A. Jiang, "Application of combined adaptive fourier filtering technique and fault detector to fast distance protection," *IEEE Transactions on Power Delivery*, vol. 21, no. 2, pp. 619–626, April 2006.